ARTICLE
Journal of Cellular Biochemistry 114:708–715 (2013)

Journal of Cellular Biochemistry

Neuroprotective Effects of PrxI Over-Expression in an in vitro Human Alzheimer's Disease Model

Annamaria Cimini,[1,2] Roberta Gentile,[1] Francesco Angelucci,[1] Elisabetta Benedetti,[1] Giuseppina Pitari,[1] Antonio Giordano,[2,3**] and Rodolfo Ippoliti[1*]

[1] *Department of Life, Health and Environmental Sciences, University of L'Aquila, L'Aquila, Italy*

[2] *Sbarro Institute for Cancer Research, Molecular Medicine, Center of Biotechnology College of Science, Technology Temple University Philadelphia, Pennsylvania 19122*

[3] *Department of Human Pathology and Oncology, University of Siena, Siena, Italy*

ABSTRACT

Peroxiredoxins are ubiquitous proteins that recently attracted major interests in view of the strict correlation observed in several cell lines and/or tissues between different levels of their expression and the increased capacity of cells to survive in different pathophysiological conditions. They are recently considered as the most important enzymes regulating the concentration of hydroperoxides inside the cells. Most of neurodisorders such as Parkinson, Huntington, Alzheimer's diseases, and ischemic injury are characterized by conditions of oxidative stress inside cells. In these pathophysiological conditions, a strict correlation between cell survival and Prx expression has been found. In CNS all the Prx isoforms are present though with different expression pattern depending on cell phenotype. Interestingly, neurons treated with amyloid beta peptide (Aβ), showed an overexpression of PrxI. In this study, the neuroprotective effect of PrxI after Aβ exposure and the underlying mechanisms by which PrxI expression counteracts cell death was investigated in a well established human AD in vitro model. Taking advantage on cells transfected by a construct where human PrxI is fused with a Green fluorescent protein (GFP) at the C-terminus, we report some events at the basis of cell survival after Aβ injury, suggesting possible new signal cascades dealing with the antiapoptotic effect of PrxI. The results obtained indicated a protective role for PrxI in counteracting Aβ injury by increasing cell viability, preserving neurites, and decreasing cell death. J. Cell. Biochem. 114: 708–715, 2013.

KEY WORDS: NEURODEGENERATION; PEROXIREDOXINS; OXIDATIVE STRESS; BDNF

Peroxiredoxins are ubiquitous proteins that recently attracted major interests in view of the strict correlation observed in several cell lines and/or tissues between different levels of their expression and the increased capacity of cells to survive in different pathophysiological conditions [Ishii et al., 2012]. In eukaryotic cells six Prx isoforms are present: four isoforms belong to the typical 2-cys Peroxiredoxin namely the cytosolic PrxI and PrxII, the mitochondrial PrxIII and PrxIV expressed in the endoplasmatic reticulum, PrxV belongs to the atypical 2-cys Prx and is mainly localized in the cytosol, mitochondria, nuclei, and peroxisomes and PrxVI which is a cytoplasmic 1-cys Prx [Nelson et al., 2011; Soito et al., 2011]. The classification is also based on the different mechanism of action in reducing peroxides involving one or two cysteines. They are recently considered as the most important enzymes regulating the concentration of hydroperoxides inside the cells [Hall et al., 2009]. In particular, 2-cys Peroxiredoxin is the largest Prx subfamily and from a cell biology point of view probably the most interesting one due to the peculiar chameleonic behavior observed for its belonging members [Nelson et al., 2011]. Under mild oxidative stress, 2-cys Prxs present peroxidase activity and use reduced thioredoxin as the electron donor to reduce organic peroxides while at higher H_2O_2 concentration they switch function acquiring molecular chaperone activity, shifting their structure toward high molecular weights species [Saccoccia et al., 2012]. This behavior is dictated by the high sensibility to inactivation by H_2O_2 due to hyperoxidation (to sulfinic/sulfonic acid, SO_2H/SO_3H) of a

Grant sponsor: Prof. Ippoliti and Prof. Cimini RIA (2011, University of L'Aquila); Dr. Angelucci and Dr. Benedetti: grant from Cassa di Risparmio dell'Aquila (CARISPAQ)

*Correspondence to: Rodolfo Ippoliti, Department of Health, Life and Environmental Sciences, University of L'Aquila, via Vetoio n 10, 67100 L'Aquila, Italy. E-mail: Rodolfo.ippoliti@univaq.it

**Correspondence to: Antonio Giordano, Department of Human Pathology and Oncology, University of Siena, Strada delle Scotte n. 6, 53100 Siena, Italy. E-mail: giordano12@unisi.it; antonio.giordano@temple.edu

Manuscript Received: 25 September 2012; Manuscript Accepted: 26 September 2012

Accepted manuscript online in Wiley Online Library (wileyonlinelibrary.com): 11 October 2012

DOI 10.1002/jcb.24412 • © 2012 Wiley Periodicals, Inc.

crucial cysteine implicated in enzyme turn-over. Considering that at low concentrations H_2O_2 is a signal molecule known to regulate cell grown and differentiation, the hampered enzymatic activity under oxidative conditions of 2-cys Prxs bears several implications in the stress and non-stress oxidative signaling [Neumann et al., 2009]. As a matter of fact, hyperoxidized 2-cys Prx has been demonstrated to play different roles in signaling: (i) As a "triage" agent, making available reduced thioredoxin to supply reducing equivalents to a redox-sensitive trascriptional factor PaP1, as recently observed in yeast [Day et al., 2012] (ii) as a peroxide "dosimeter" able to regulate cell cycle [Phalen et al., 2006] and (iii) as a "floodgate" where, upon its inactivation, local increments of H_2O_2 for signal purposes become available [Hall et al., 2009]. In eukaryotic cells, Prx hyperoxidation and, consequently, the arising signaling events are reversed by the action of sulfiredoxin, an enzyme able to restore the normal condition of Prx reducing sulfinic acid state of its catalytic cysteine [Lowther and Haynes, 2011].

By this scenario is not surprising that 2-Cys Prxs are known to regulate mitogen-activated protein kinase activity and to modulate the activity of NF-kB, a crucial transcription factor [Barford, 2004; Kang et al., 2004; Veal et al., 2004]. More in general their action has been associated with various cellular phenomena, including cell proliferation, differentiation, immune responses, tumorigenesis, and apoptosis. Relatively to the latter process, hyperoxidized human PrxII has been demonstrated to be cytoprotective in HeLa cells subjected to oxidative conditions due its capacity to counteract the H_2O_2-induced apoptosis [Moon et al., 2005].

Most of neurodisorders such as Parkinson [Lee et al., 2008], Huntington [Pitts et al., 2012], Alzheimer's diseases [Sultana and Butterfield, 2010; Cai et al., 2011], and ischemic injury [Gan et al., 2012] are characterized by conditions of oxidative stress inside cells. In these pathophysiological conditions, a strict correlation between cell survival and Prx expression has been found [Lee et al., 2008; Pitts et al., 2012; Cumming et al., 2007; Gan et al., 2012; Zhu et al., 2012]. In CNS all the Prx isoforms are present though with different expression pattern depending on cell phenotype. PrxI and IV were constitutively expressed in glial cells but not in neurons, whereas PrxII, III, IV, and V were expressed in neurons [Goemaere and Knoops, 2012]. Interestingly, neurons treated with amyloid beta peptide (Aβ), showed an overexpression of PrxI. In these conditions, PrxI is only moderately hyperxodized, while PrxII is mainly found in this form [Cumming et al., 2007]. This finding supports the reported protective role of PrxI when transfected in PC12 cells or in primary hippocampal neurons subjected to Aβ exposure [Cumming et al., 2007]. Transfection recovers neurons from injury and likely triggers stress oxidative signaling which maintain cell viability [Cumming et al., 2007]. Furthermore, it has been recently demonstrated that treatments with antioxidant substances such as cerium oxide nanoparticles or flavonoids [D'Angelo et al., 2009; Cimini et al., 2012; Cimini et al., ms submitted] can induce neuroprotection in SH-S5SY cell line against amyloid injury; moreover, it has been shown that compounds as salidroside (a component of an erbal extract from a chinese plant, Rhodiola rosea L.) may be neuroprotective due, among the various effects, to the upregulation of the expression of Prx1 gene [Zhang et al., 2010]. Cumming et al. [2007] also reported an increase of Prx1 expression in AD patient's cortical samples and the overexpression of the same protein in PC12 neuronal clones resistant to amyloid treatments.

The antiapoptotic effect of 2-cys Prxs demonstrated in HeLa cells, but also in pancreatic β cells and in cardiomyocytes and their neuroprotective role observed in neurons exposed to Aβ injury, inspires this study which investigates in a well established human in vitro AD model [D'Angelo et al., 2009; Cimini et al., 2012], the neuroprotective effect of PrxI after Aβ exposure and the underlying mechanisms by which PrxI expression counteracts the induced cell death. Taking advantage on cells transfected by a construct where human PrxI is fused with a Green fluorescent protein (GFP) at the C-terminus we shed light on some events at the basis of cell survival after Aβ injury suggesting possible new signal cascades dealing with the antiapoptotic effect of PrxI. The results obtained indicated a protective role for Prx1 in counteracting Aβ injury by increasing cell viability, preserving neurites, and decreasing cell death.

MATERIALS AND METHODS

MATERIALS

Triton X-100, dimethylsulfoxide (DMSO), sodium dodecylsulfate (SDS), Tween20, bovine serum albumine (BSA), L-glutamine, 4′,6 diamino-2-phenylindole dilactate (DAPI), Nonidet P40, sodium deoxycolate, ethylen diamine tetraacetate (EDTA), phenylmethanesulphonylfluoride (PMSF), sodium fluoride, sodium pyrophosphate, orthovanadate, leupeptin, aprotinin, pepstatin, NaCl, polyvinylidene difluoride (PVDF) sheets, fluorescein-labeled anti-rabbit and antimouse IgG antibodies, mouse anti-GAP 43, anti-heavy neurofilament (NF-H), anti P 75 NTR antibodies, Aβ (25–35), and Aβ (1–42) were all purchased from Sigma Chemical Co (St. Louis, CO). Trypsin-EDTA solution, N2 supplement, streptomycin–penicillin were from Gibco Invitrogen GmbH (Austria); Mouse anti p-ERK1/2, rabbit anti-ERK1, rabbit anti-BDNF, rabbit anti-TrkB, anti-caspase 3 antibodies, horseradish peroxidase (HRP)-conjugated anti-rabbit, and anti-mouse for were from St. Cruz Biotechnology (Santa Cruz, CA); mouse anti-β-tubulin III antibody was from Promega (Mannheim, Germany); rabbit anti-Pospho Ras/extracellular signal-regulated kinase 5 (pERK5) antibodies was purchased from Upstate, Millipore S.p.A (Milan, Italy). RPMI-1640 medium and fetal bovine serum (FBS) ware from Euroclone Ltd (UK); Apoptosis assay kit were from Roche Diagnostic (Indianapolis, IN). Micro BCA protein detection kit from Pierce (Rockford, IL). Vectashield was purchased from Vector Laboratories (Burlingame, CA). All other chemicals were of the highest analytical grade.

Cell Cultures. SH-SY5Y cells (ATCC) were seeded at 1×10^4 cells/cm^2 cultured for 7 DIV in FBS-free RPMI 1640 differentiating medium containing N2 supplement in order to allow the neuronal differentiation.

Aβ Fibril Formation. Aβ (25–35) is frequently used in investigating Aβ properties as a less expensive and more easily handled substitute for the native full-length peptide, Aβ(1–42). Indeed, Aβ (25–35) mimics the toxicological and aggregation properties of the full-length peptide, though these characteristics are enhanced; i.e., the shorter peptide is more toxic to cultured neurons, exhibits earlier toxicity, causes more severe membrane protein oxidation, and aggregates faster than the native Aβ (1–42) [Santos

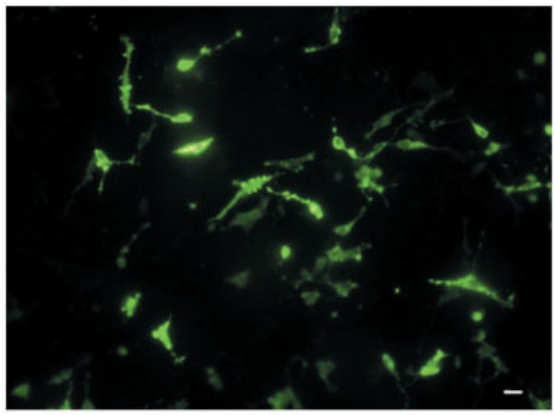

Fig. 1. Fluorescence microscopy of differentiated transfected cells probed by GFP. Bar = 17 μm.

et al., 2005]. The amyloid fibrils were obtained as previously described [Varadarajan et al., 2001]. Specifically, the Aβ (25–35) stock solution (500 μM) was prepared dissolving Aβ in FBS-free differentiating medium containing N2 supplement (pH 7.4) and stored at −20°C. The amyloid fibrils were obtained incubating Aβ (25–35) stock solution at 37°C for 8 days.

Fluorimetric Assay. The amyloid polymerization status was checked by the thioflavin T (ThT) fluorescence method before each treatment [Santos et al., 2005]. ThT binds specifically to amyloid fibrils, and such binding produces a shift in its emission spectrum and an increase in the fluorescent signal, which is proportional to the amount of amyloid formed [Naiki et al., 1991; Muñoz and Inestrosa, 1999]. Following incubation, Aβ in 20 mM Tris HCl Buffer, pH 8.0, and 1.5 μM ThT in a final volume of 2 ml were analyzed. Fluorescence was monitored at excitation wavelength of 450 nm and emission of 485 nm by spectrofluorimetry, as previously described [Inestrosa et al., 1996].

Transfection. One day before transfection, 0.5–2 × 10^5 cells were plated in 500 μl of growth medium without antibiotics until the reaching of 90–95% confluence. For each transfection sample, complexes were prepared as follows: 0.2–4 μg DNA were diluted in 250 μl of DMEM containing Glutamine. 0.5–10 μl Lipofectamine™ 2000 (Invitrogen) were mixed gently before use and then diluted in 250 μl of DMEM with Glutamine. After 5 min of incubation at RT the diluted DNA was combined with diluted Lipofectamine™ 2000 (total volume = 500 μl) and incubated for 20 min at room temperature. The complex solutions were added to each well containing cells and incubated at 37°C in a CO_2 incubator for 18–48 h prior to testing for transgene expression. Medium was changed after 6 h.

Cell Viability and death. Cells, plated on 24 multiwell plates, were incubated, after treatments, for 2 h with CellTiter 96 AQ_{ueous} One Solution, a colorimetric method based on 3-(4,5-dimethylthiazol-2-yl)-5-(3-carboxymethoxyphenil)-2-(4-sulfophenyl)-2H-tetrazolium (MTS). The quantity of formazan formed, as a function of viability, was measured at 490 nm using an ELISA plate reader. All MTS assays were performed in triplicate.

For apoptosis detection, cells were seeded in 24-well plates at a density of 1 × 10^4 cells/cm^2. Control and treated cells were analyzed for apoptosis using the Cell death detection ELISA kit for the nucleosome detection. Absorbances at 405 nm with respect to 490 nm were recorded according to manufacturer's directions.

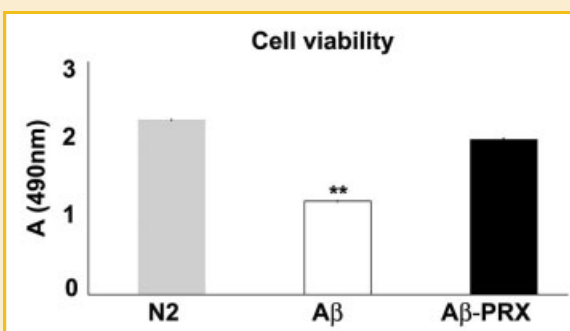

Fig. 2. Cell viability, evaluated by MTS assay, in N2 differentiated, Aβ treated (Aβ) cells and Aβ-Prxl-treated cells. Data are means ± SE; $^{**}P \leq 0.005$; $^{*}P < 0.05$.

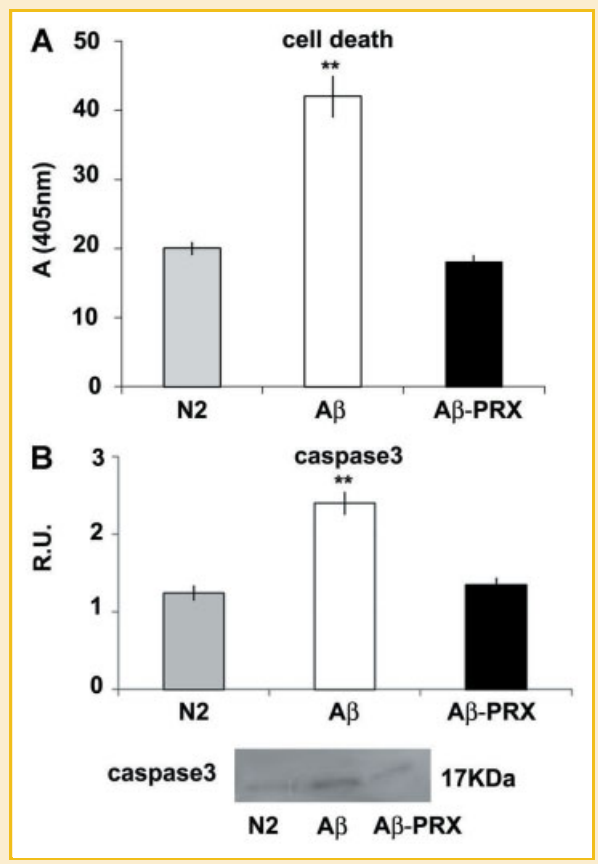

Fig. 3. Apoptotic cell death, evaluated as nucleosome concentration, in N2 differentiated, Aβ treated (Aβ) cells and Aβ-Prxl-treated cells. Data are means ± SE; $^{**}P \leq 0.005$; $^{*}P < 0.05$. In the bottom, western blotting analysis for caspase 3. Data are means ± SE; $^{**}P \leq 0.005$; $^{*}P < 0.05$.

After Aβ exposure, cells on coverslips were fixed in 4% paraformaldehyde at room temperature for 10 min, then stained with DAPI (300 ng/ml) for 20 min and examined under UV illumination, using a fluorescence microscope. To quantify the apoptotic process, nuclei with both fragmented or condensed DNA and normal DNA were counted. Five fields/coverslips were counted. Data are expressed as a percentage of the total cells counted.

Morphometry. Control and treated cells, grown on coverslips, were fixed in 4% paraformaldehyde in PBS for 20 min at RT. After washings, coverslips were mounted with Vectashield and phase-contrast observations were performed by an AXIOPHOT Zeiss microscope, equipped with a micrometric ocular lens. The processes longer than the cell body mean diameter (Ø), which should be regarded as neurites, were counted and the results were expressed as neurites number versus the total cell number. The neurite length was determined by comparing the neurite length with the mean diameter (Ø) of cell soma and reported as neurite length/soma (Ø).

Immunofluorescence. Control and treated cells, grown on coverslips, were fixed with absolute methanol for 10 min at −20°C. After that, cells were rehydrated with PBS for 5 min and incubated with anti-β tubulin III (1:300) antibody, overnight at 4°C. After extensive washings with PBS, cells were treated with Tritc-labeled anti-rabbit IgG secondary antibodies (1:100 in PBS containing 3% BSA) for 30 min at RT. Nuclei were counterstained with DAPI (300 ng/ml). After extensive washings, coverslips were mounted with Vectashield mounting medium and photographed in a fluorescence microscope (AXIOPHOT, Zeiss).

Western Blot. Cells were washed in ice-cold PBS and homogenized in ice-cold RIPA buffer (10 mM Hepes, pH7.4, 10 mM KCl, 1.5 mM MgCl2, 1 mM EDTA, 1 mM dithiothreitol) with a protease inhibitor mixture (100 mg/ml phenylmethylsulfonyl fluoride, 2 mg/ml aprotinin, 2 mM leupeptin, and 1 mg/ml pepstatin). The lysate was subjected to centrifugation at 600*g* for 30 min at 4°C, and the supernatant was collected. Samples (25–50 μg/lane) were analyzed by 10% SDS–PAGE, transferred to PVDF membranes, and blocked in Tris-buffered saline containing 5% non fat milk, and 0.1% Tween 20. Membranes were incubated with different primary antibodies, anti-BDNF (1:200), anti TrkB (1:200), anti p-75 NTR

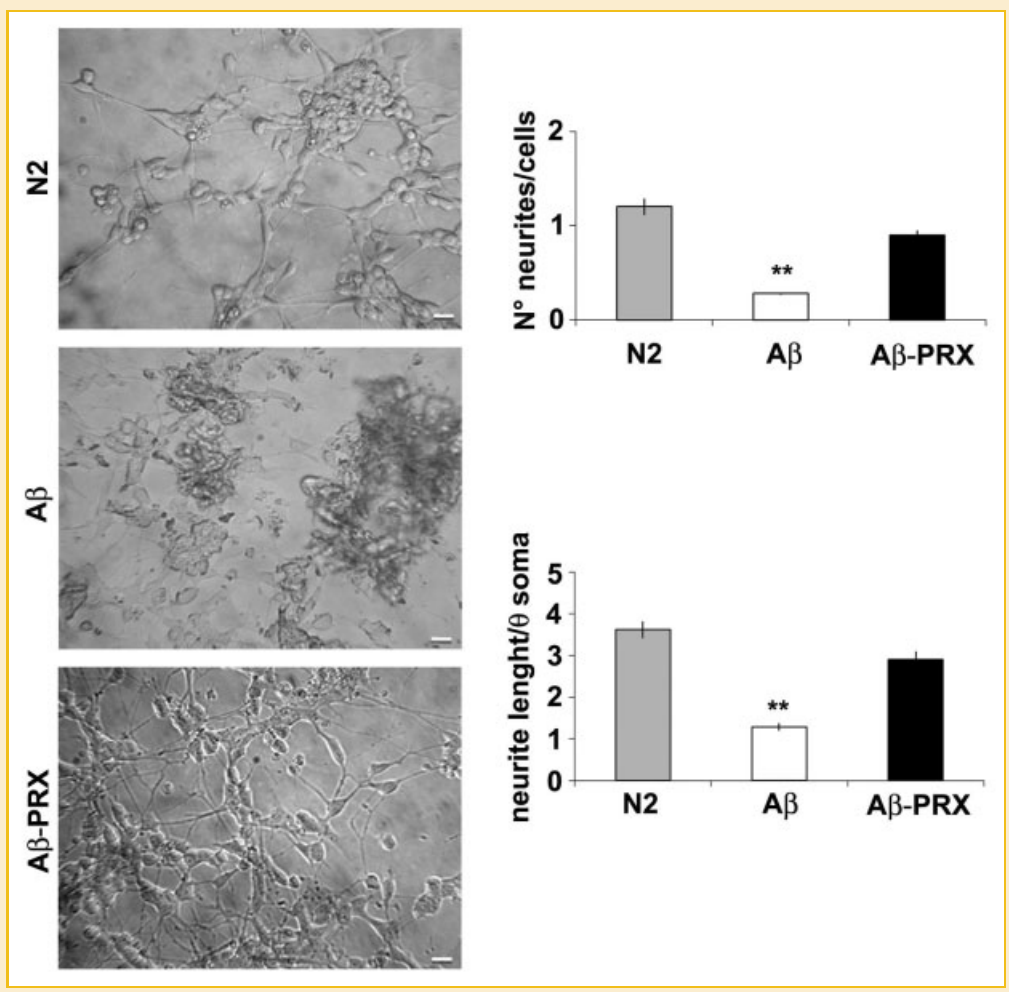

Fig. 4. Phase-contrast microscopy in N2 differentiated, Aβ treated (Aβ) cells and Aβ-PrxI-treated cells. Bar 17 μm; at the bottom the neurite number and length in N2 differentiated, Aβ treated cells and Aβ-PrxI-treated cells. Histograms report n°-neurites/n°-cells. The neurite length was determined as neurite lenght/Ø soma. Data are means ± SE; $^{**}P \leq 0.005$; $^{*}P < 0.05$.

(1: 100), anti p-ERK1,2 (1:200), anti-p-ERK5 (1:200), anti-Caspase3 (1:500) overnight at 4°C and then probed with horseradish peroxidase-conjugated mouse or rabbit secondary antibodies (1:1,000). Immunoreactive bands were visualized by chemiluminescence. Band relative densities, against most evident band of PVDF membrane Comassie Blu stained, were determined using TotalLab software (ABEL Science-Ware srl, Italy) and values were given as relative units.

Statistics. Experiments were performed at least in triplicates. Data were represented as means ± Standard Errors. Where appropriate, one-way ANOVA test followed by Scheffe's "post hoc test" analysis was performed using SPSS software. *P*-values less than 0.05 were considered statistically significant.

RESULTS

Figure 1 reports PrxI transfection evaluated by fluorescence microscopy, looking at the GFP emission. On the basis of GFP-positive cells, we estimate a high degree of transfection (about 30%), as already reported by Dalby et al. [2004].

In Figure 2 cell viability, evaluated by MTT assay, in N2 differentiated, Aβ-treated, and Aβ-PRX1 cells is shown. In agreement with previous experiments Aβ induced a decrease of cell viability [D'Angelo et al., 2009; Cimini et al., 2009; Cimini et al., 2012], while PrxI transfection was able to significantly protect cells from Aβ injury, as previously observed by Cumming et al. [2007].

In Figure 3 cell death, evaluated as nucleosome concentration, in N2 differentiated, Aβ-treated, and Aβ-PrxI cells is reported. Aβ treatment induced a significant increase of apoptosis while the concomitant presence of PrxI counteracted apoptosis promotion by Aβ. In the same picture caspase 3 activation, evaluated in western blotting, is also shown. In agreement with the pro-apoptotic effect observed by cytoplasmic nucleosome concentration, Aβ treatment induced caspase 3 activation, while PrxI presence maintained caspase levels to those of control cells.

Figure 4 shows contrast phase microscopy, the graphic representation of neurite length and the number of neurites in N2 differentiated, Aβ-treated, and Aβ-PrxI cells. Control cells (N2) show an evident neuronal clustering and neuronal aggregation, while Aβ treatment induced an evident neurite loss (Aβ). PrxI transfection protects cells from Aβ-induced neurite atrophy. The graphical representation of neurite number, and neurite length shows that Aβ treatment significantly decreases neurite number and also the neurite length, while PrxI protects the neurites from Aβ-mediated neuronal damage.

Since neuronal loss and neuritic/cytoskeletal lesions (synaptic disconnection and proliferation of dystrophic neurites) represent the major dementia-associated abnormalities in AD, early neuronal differentiation marker localization, such as β-tubulin III was investigated in control and treated cells (Fig. 5). In control cells

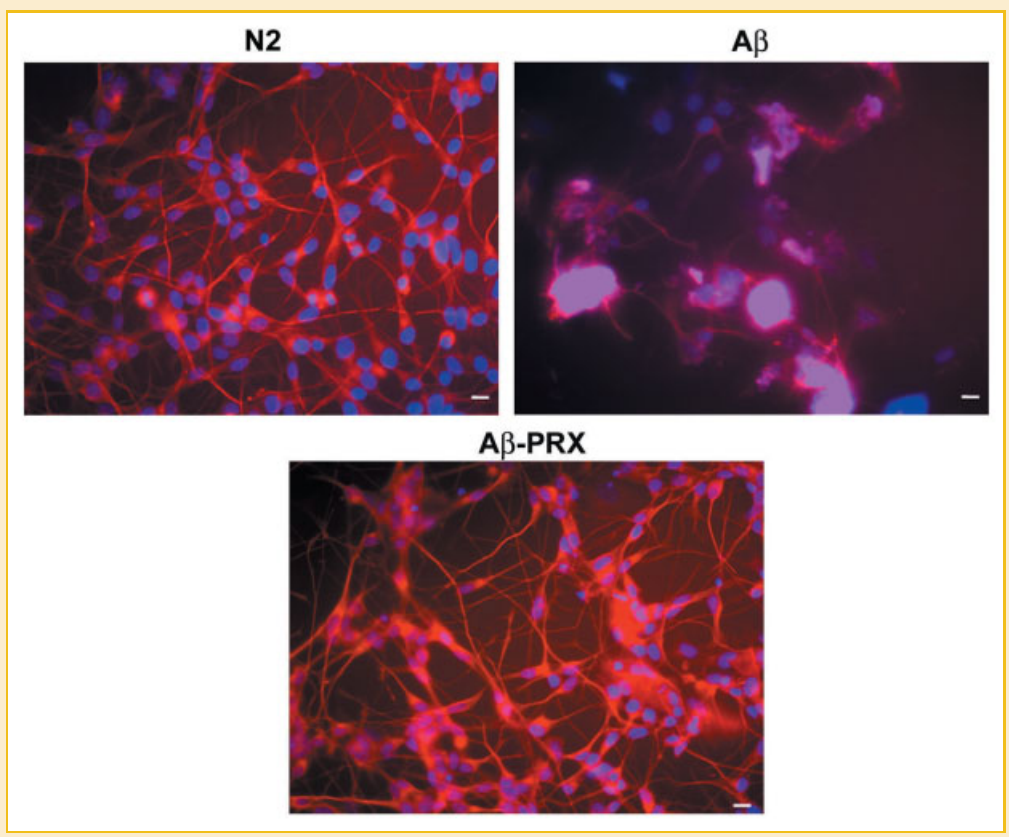

Fig. 5. β-tubulin III immunolocalization in N2 differentiated, Aβ treated (Aβ) cells, and Aβ-PrxI-treated cells. Bar 17 μm.

β-tubulin III localization shows an organized cytoskeletal structure that is lost after Aβ treatment, where a significant decrease of neurite branching is observed. PrxI preserved cytoskeletal organization, thus confirming its neuroprotective effects in counteracting neuronal dystrophy.

The signal transduction pathways involved in neuronal survival, neurotrophines modulation, and neuronal death were investigated in control and treated cells (Fig. 6). Brain Derived Neurotrophic Factor (BDNF) is a neurotrophin involved in neuronal survival and differentiation, affecting neuronal morphology and plasticity. Its activity is mediated by the high affinity receptor TrkB and by the low affinity receptor p75NTR.

Therefore we assayed the BDNF, its receptors such as TrkB and p75, and the extracellular signal regulated kinases such as ERK1,2 and ERK5. Upon Aβ challenge, the cytoplasmatic levels of BDNF immature form (pro-BDNF) appear upregulated (Fig. 6). This strong increase of pro-BDNF may be responsible for the promotion of the neuronal death and atrophy, as it is known that the immature form of BDNF induces neuronal apoptosis via activation of a receptor complex of p75NTR and sortilin [Teng et al., 2005]. This notion is supported by the results obtained for p75NTR protein in our experimental condition (Fig. 6). In fact, as for pro-BDNF, Aβ increases p75NTR protein levels while concomitantly triggers a decrease of the specific receptor TrkB (Fig. 6) involved in the action of mature and cleaved form of BDNF. Moreover Aβ induces the upregulation of the active form of ERK1,2 (p-ERK1,2) and of JNK (Fig. 7), both known to be involved in apoptosis promotion, and a downregulation of ERK5 (Fig. 7), involved in neuronal survival. In Aβ-treated cells transfected with PrxI a complete reversion of pro-BDNF levels is observed (Fig. 6). In the same time, the overespression of PrxI, significantly increase TrkB as well as p-ERK5 (Figs. 6 and 7, respectively), involved in neuronal survival, with concomitant decrease of p-ERK1,2 and p-JNK (Fig. 7), suggesting an activation of the neuronal survival pathway BDNF/TrkB/ERK5 in the presence of PrxI.

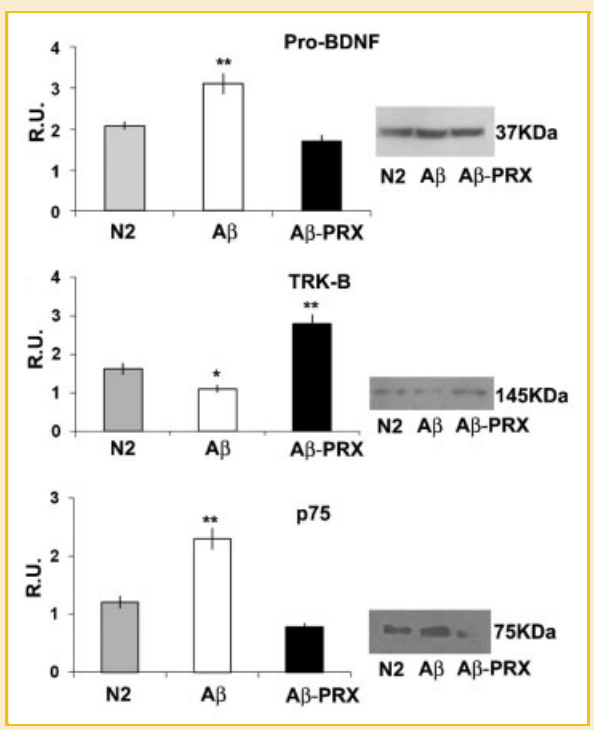

Fig. 6. Western blotting and densitometric analyses for TrkB, P75NTR, and cytoplasmatic pro-BDNF, in N2 differentiated, Aβ treated (Aβ) cells and Aβ-PrxI-treated cells. Band relative densities, were determined against most evident band of PVDF membrane Comassie Blu stained. Data are means ± SE, $^{**}P \leq 0.005$; *, $P < 0.05$.

DISCUSSION

Oxidative stress is considered as a risk factor in the incidence and progression of cognitive declines that occur during normal cerebral aging and dementia and plays a critical role in many neurodegenerative processes, such as AD and Parkinson's disease [Selkoe, 2002; Selkoe, 2004]. Recently, a role for Prxs has been proposed in neurodegenerative diseases such as Alzheimer's and Parkinson diseases [Zhu et al., 2012]. Specifically, it has been demonstrated that both in aging and in neurodegeneration, the neuronal isoform PrxII, is significantly downregulated in hippocampus and *substantia nigra*, the brain areas involved in pathologies such as AD and PD, which are endowed by very low basal levels of Prxs [Zhu et al., 2012].

PrxI transfection has been previously demonstrated to protect PC12 cell viability against Aβ injury [Cumming et al., 2007]. In this work we demonstrated, for the first time, in an in vitro human AD model, that PrxI transfection in differentiated neurons challenged with Aβ25–35, protects cells from the hallmarks of AD such as neurite dystrophy and cell death. While increasing survival, PrxI promotes the maintenance of neuronal network as evaluated by neurites length and number and by the expression and localization of the cytoskeleton protein β-tubulin III.

Upon Aβ challenge, pro-BDNF, p-ERK1,2, and p-JNK appear all increased and this effect may be related to the known "dark side" effect of pro-BDNF under oxidative stress conditions [D'Angelo et al., 2009]: Pro-BDNF may activate, through p-75 and sortilin, ERK1,2, and JNK which, in AD, has been involved in apoptotic neuronal death [Teng et al., 2005]. Moreover, Aβ slightly decreased also the active form of ERK5, involved in neuronal survival. On the other hand, BDNF is known to be effective in the promotion of neuronal survival in the presence of anti-oxidants. In this view, PrxI, by decreasing pro-BDNF and p75NTR and increasing TrkB and ERK5 levels, tries to counteract neuronal death and to promote cell survival, since Aβ plaques are, however, present in PrxI transfected cells.

The results obtained appear original since demonstrate that PrxI is not per se a simple anti-oxidant agent, but it affects, directly or indirectly, likely by modulating oxidative stress, signal transduction pathways involved in neuronal death and neuroprotection. Indeed, it has been already demonstrated that PrxI can act along the response to oxidative pathways modulating the response to hydrogen peroxide, as a function of the concentration of this molecule and in response to growth factors [Kang et al., 1998].

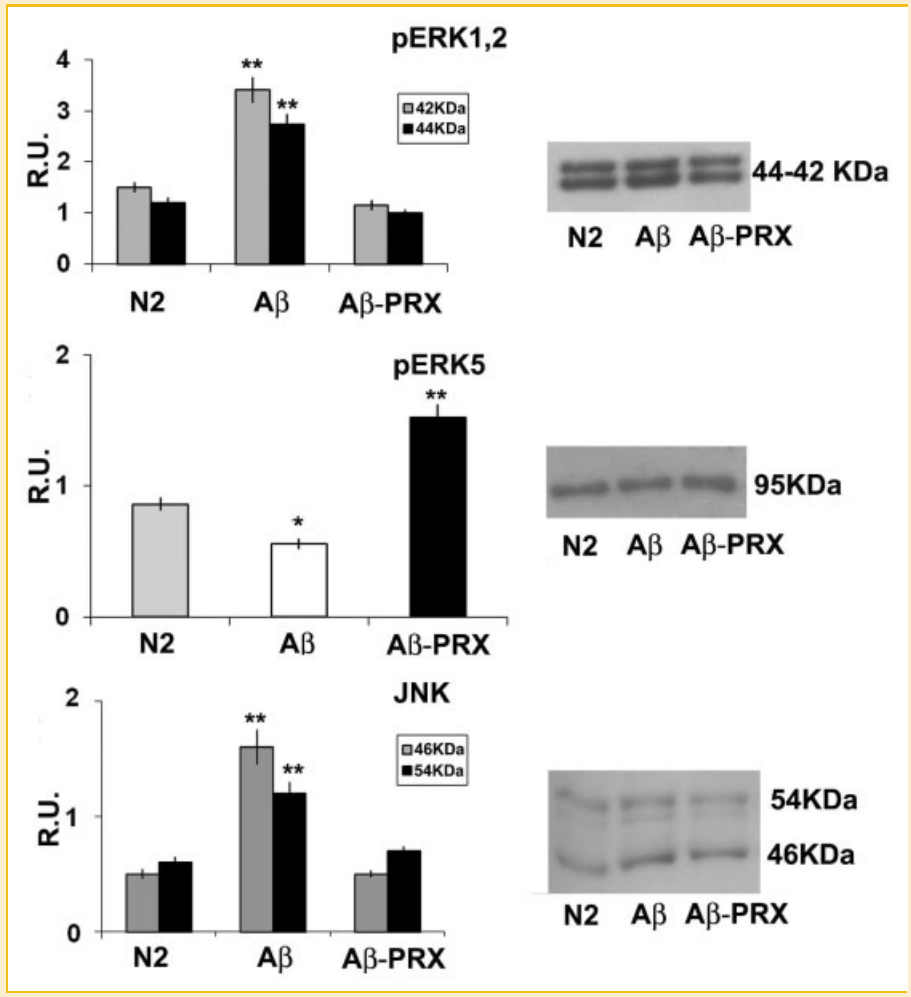

Fig. 7. Western blotting and densitometric analyses for p-ERK1,2 p-ERK5, and p-JNK in N2 differentiated, Aß treated (Aß) cells and Aβ-PrxI-treated cells. Band relative densities, were determined against most evident band of PVDF membrane Comassie Blu stained. Data are means ± SE; $^{**}P \leq 0.005$; $^{*}P < 0.05$.

PrxI is deeply involved in a fine tuning of the cellular responses to oxidative stress, thus supporting our results and indicating the possibility of its use as treatment for cell-based therapy for neurodegenerative diseases characterized by oxidative stress.

REFERENCES

Barford D. 2004. The role of cysteine residues as redox-sensitive regulatory switches. Curr Opin Struct Biol 14:679–686.

Cai Z, Zhao B, Ratka A. 2011. Oxidative stress and β-amyloid protein in Alzheimer's disease. Neuromolecular Med 13:223–250.

D'Angelo B, Santucci S, Benedetti E, Di Loreto S, Phani RA, Falone S, Amicarelli F, Cerù MP, Cimini A. 2009. Cerium oxide nanoparticles trigger neuronal survival in a human Alzheimer disease model by modulating BDNF pathway. Curr Nanosci 5:167–176.

Cimini A, Benedetti E, D'Angelo B, Cristiano L, Falone S, Di Loreto S, Amicarelli F, Cerù MP. 2009. Neuronal response of peroxisomal and peroxisome-related proteins to chronic and acute Abeta injury. Curr Alzheimer Res 6:238–251.

Cimini A, D'Angelo B, Das S, Gentile R, Benedetti E, Singh V, Monaco AM, Santucci S, Seal S. 2012. Antibody-conjugated PEGylated cerium oxide nanoparticles for specific targeting of Aβ aggregates modulate neuronal survival pathways. Acta Biomater 8:2056–2067.

Cumming RC, Dargusch R, Fischer WH, Schubert D. 2007. Increase in expression levels and resistance to sulfhydryl oxidation of peroxiredoxin isoforms in amyloid beta-resistant nerve cells. J Biol Chem 282:30523–30534.

Dalby B, Cates S, Harris A, Ohki EC, Tilkins ML, Price PJ, Ceccarone VC. 2004. Advanced transfection with lipofectamine 2000 reagent: Primary neurons, SiRNA, and high-troughput applications. Methods 33:95–103.

Day AM, Brown JD, Taylor SR, Rand JD, Morgan BA, Veal EA. 2012. Inactivation of a peroxiredoxin by hydrogen peroxide is critical for thioredoxin-mediated repair of oxidized proteins and cell survival. Mol Cell 45:398–408.

Gan Y, Ji X, Hu X, Luo Y, Zhang L, Li P, Liu X, Yan F, Vosler P, Gao Y, Stetler RA, Chen J. 2012. Transgenic Overexpression of Peroxiredoxin-2 Attenuates Ischemic Neuronal Injury Via Suppression of a Redox-Sensitive Pro-Death Signaling Pathway. Antioxid Redox Signal 17:719–732.

Goemaere J, Knoops B. 2012. Peroxiredoxin distribution in the mouse brain with emphasis on neuronal populations affected in neurodegenerative disorders. J Comp Neurol 520:258–280.

Hall A, Karplus PA, Poole LB. 2009. Typical 2-Cys peroxiredoxins–structures, mechanisms and functions. FEBS J 276:2469–2477.

Inestrosa NC, Alvarez A, Perez CA, Moreno RD, Vicente M, Luker C, Casanueva OI, Soto C, Garrido J. 1996. Acetylcholinesterase accelerates assembly of amyloid-[beta]-peptides into Alzheimer's fibrils: Possible role of the peripheral site of the enzyme. Neuron 16:881–891.

Ishii T, Warabi E, Yanagawa T. 2012. Novel roles of peroxiredoxins in inflammation, cancer and innate immunity. J Clin Biochem Nutr 50:91–105.

Kang SW, Chae HZ, Seo MS, Kim K, Baines IC, Rhee SG. 1998. Mammalian peroxiredoxin isoforms can reduce hydrogen peroxide generated in response to growth factors and tumor necrosis factor-alpha. J Biol Chem 273:6297–6302.

Kang SW, Chang TS, Lee TH, Kim ES, Yu DY, Rhee SG. 2004. Peroxiredoxin II restrains DNA damage-induced death in cancer cells by positively regulating JNK-dependent DNA repair. J Biol Chem 279:2535–2543.

Lee YM, Park SH, Shin DI, Hwang JY, Park B, Park YJ, Lee TH, Chae HZ, Jin BK, Oh TH, Oh YJ. 2008. Oxidative modification of peroxiredoxin is associated with drug-induced apoptotic signaling in experimental models of Parkinson disease. J Biol Chem 283:9986–9998.

Lowther WT, Haynes AC. 2011. Reduction of cysteine sulfinic acid in eukaryotic, typical 2-Cys Peroxiredoxins by Sulfiredoxin. Antioxid Redox Signal 15:99–109.

Moon JC, Hah YS, Lim WY, Young HH, Lee JR, Kim SY, Lee YM, Jeon MG, Kim CW, Cho MJ, Lee SY. 2005. Oxidative stress-dependent structural and functional switching of a human 2-Cys peroxiredoxin isotype II that enhances HeLa cell resistance to H2O2-induced cell death. J Biol Chem 280:28775–28784.

Muñoz FJ, Inestrosa NC. 1999. Neurotoxicity of acetylcholinesterase amyloid betapeptide aggregates is dependent on the type of Abeta peptide and the AChE concentration present in the complexes. FEBS Lett 450: 205–209.

Naiki H, Higuchi K, Nakakuki K, Takeda T. 1991. Kinetic analysis of amyloid fibril polymerization in vitro. Lab Invest 65:104–110.

Nelson KJ, Knutson ST, Soito L, Klomsiri C, Poole LB, Fetrow JS. 2011. Analysis of the peroxiredoxin family: Using active-site structure and sequence information for global classification and residue analysis. Proteins 79:947–964.

Neumann CA, Cao J, Manevich Y. 2009. Peroxiredoxin I and its role in cell signaling. Cell Cycle 8:4072–4078.

Phalen TJ, Weirather K, Deming PB, Anathy V, Howe AK, van der Vliet A, Jönsson TJ, Poole LB, Heintz NH. 2006. Oxidation state governs structural transitions in peroxiredoxin II that correlate with cell cycle arrest and recovery. J Cell Biol 175:779–789.

Pitts A, Dailey K, Newington JT, Chien A, Arseneault R, Cann T, Thompson LM, Cumming RC. 2012. Dithiol-based compounds maintain the expression of the antioxidant protein Peroxiredoxin 1 which counteracts the toxicity of mutant Huntingtin. J Biol Chem 287:22717–22729.

Saccoccia F, Di Micco P, Boumis G, Brunori M, Koutris I, Miele AE, Morea V, Sriratana P, Williams DL, Bellelli A, Angelucci F. 2012. Moonlighting by different stressors: Crystal structure of the chaperone species of a 2-Cys peroxiredoxin. Structure 20:429–439.

Santos MJ, Quintanilla RA, Toro A, Grandy R, Dinamarca MC, Godoy JA, Inestrosa NC. 2005. Peroxisomal proliferation protects from β-amyloid neurodegeneration. J Biol Chem 280:41057–41068.

Selkoe DJ. 2002. Alzheimer's disease is a synaptic failure. Science 298:789–791.

Selkoe DJ. 2004. Cell biology of protein misfolding: The examples of Alzheimer's and Parkinson's diseases. Nat Cell Biol 6:1054–1061.

Soito L, Williamson C, Knutson ST, Fetrow JS, Poole LB, Nelson KJ. 2011. PREX: PeroxiRedoxin classification indEX, a database of subfamily assignments across the diverse peroxiredoxin family. Nucleic Acids Res 39:D332–D337.

Sultana R, Butterfield DA. 2010. Role of oxidative stress in the progression of Alzheimer's disease. J Alzheimers Dis 19:341–353.

Teng HK, Teng KK, Lee R, Wright S, Tevar S, Almeida RD, Kermani P, Torkin R, Chen ZY, Lee FS, Kraemer RT, Nykjaer A, Hempstead BL. 2005. ProBDNF Induces Neuronal Apoptosis via Activation of a Receptor Complex of p75NTR and Sortilin. J Neurosci 25:5455–5463.

Varadarajan S, Kanski J, Aksenova M, Lauderback C, Butterfield DA. 2001. Different mechanisms of oxidative stress and neurotoxicity Alzheimer's A beta(1–42) and A beta (25–35). J Am Chem Soc 123:5625–5631.

Veal EA, Findlay VJ, Day AM, Bozonet SM, Evans JM, Quinn J, Morgan BA. 2004. A 2-Cys peroxiredoxin regulates peroxide-induced oxidation and activation of a stress-activated MAP kinase.Mol. Cell 15:129–139.

Zhang L, Yu H, Zhao X, Lin X, Tan C, Cao G, Wuang Z. 2010. Neuroprotective effects of salidroside against ß-amyloid-induced oxidative stress in SHSY5Y human neuroblastoma cells. Neurochem Int 57:547–555.

Zhu H, Santo A, Li Y. 2012. The antioxydant enzyme peroxiredoxin and its protective role in neurological disorders. Exp Biol Med 237:143–149.